Journal of Engineering Physics and Thermophysics, Vol. 73, No. 4, 2000

RESPONSE OF A PLIABLE COATING TO TURBULENT PRESSURE PULSATIONS

V. M. Kulik, S. L. Morozova, and S. V. Panov

UDC 532.526.4:539.3

The duration of the portions of coherence of turbulent pressure pulsations is determined experimentally. Based on this the dimensionless rate of deformation of the surface of a pliable coating is calculated with allowance for its inertial properties.

Interest in studying pliable coatings was provoked by a series experiments of Kramer [1]. His coatings imitated the skin of dolphins, which can swim at an abnormally high speed. Kramer assumed that the coating damps Tollmin–Schlichting waves and thereby delays the transition to turbulence.

Benjamin [2] assumed that a pliable coating can reduce friction in turbulent flow, modifying its boundary layer, but the character of the flow itself remains turbulent. Indeed, in Kramer's experiments, too, the turbulent friction was, apparently, reduced since there was a turbulizer in the forepart of his model. Many schemes of pliable coatings, a classification of which is proposed in [3], have been put forward and tested in the ensuing years. The greatest attention was paid to passive coatings deformed by turbulent pressure pulsations.

To explain the friction reduction in a developed turbulent flow, two hypotheses have currently been developed. The first considers the propagation of deformation waves over the coating surface that are caused by the pressure pulsations on the wall. The friction reduction is associated with energy dissipation inside the wall. In the most developed theory [4], one predicts parameters of the coating material for which unstable deformations of the surface do not occur.

The second theory [5] assumes that the coating is locally deformable. This means that running waves do not propagate from the site of application of the periodic deformation. The friction reduction is related to a change in the pattern of generation of Reynolds stresses $\langle \rho uv \rangle$ in the wall region. Such a change is quite possible, since the component of the pulsating velocity v that is normal to the wall can change in both magnitude and phase because of deformation of the wall by the turbulent pressure pulsations. So far, neither theory can calculate the friction reduction; they are capable only of predicting the region of the parameters of the coating material where friction reduction is possible.

In [6], a material whose properties are calculated according to the Duncan theory is used and a decrease in the turbulence intensity, coefficient of friction, and Reynolds stresses is obtained. Coatings calculated according to the Semenov theory turned out to be much more rigid but showed a decrease of up to $\approx 17\%$ in the friction and the level of pressure pulsations [7]. Tests of these coatings in a cavitation tunnel at the University of Newcastle carried out by independent researchers [8] using more sophisticated measuring equipment confirmed the validity of the previous neasurements.

Thus, there are two alternatives at present: "soft" coatings with running waves and locally deformable "rigid" coatings. To describe the operation of both coatings, we must know the manner in which the coating surface is deformed under the action of turbulent pressure pulsations. The dependence of the deformation on the applied pulsating pressure is always assumed to be linear. The proportionality factor is called the pliability of the coating (the reciprocal is the rigidity). A second important parameter is the phase angle by which the deformation lags behind the pressure.

Institute of Thermal Physics, Siberian Branch of the Russian Academy of Sciences, Novosibirsk, Russia. Translated from Inzhenerno-Fizicheskii Zhurnal, Vol. 73, No. 4, pp. 712-718, July–August, 2000. Original article submitted January 15, 1999; revision submitted July 30, 1999.

1062-0125/00/7304-0699$25.00

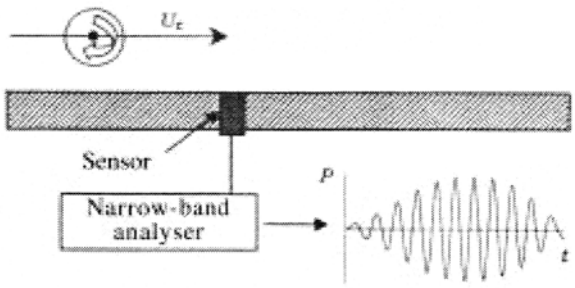

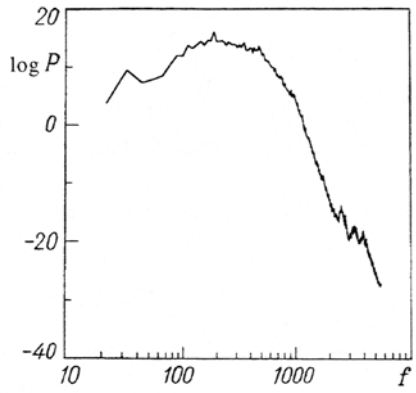

Fig. 1. Measuring scheme.

Fig. 2. Fourier spectrum. *f*, Hz.

These vibrational characteristics can be measured directly [9]; however one usually calculates them [10, 11].

Only a steady regime of deformation was dealt with in all previous works. However pressure pulsations taken in a rather narrow frequency band, for example, in the region of the pliability peak, have a variable amplitude level. The envelope of this signal is dome-shaped and is related to passage of a vortex structure by the observation point, as shown in Fig. 1 [12]. This important fact was taken into account by Duncan [13] when the wave pattern of deformation of a monolithic coating was calculated.

However a pliable coating, by virtue of its inertial properties (for example, the presence of an inertial mass, a spring, and a damper in the Voigt and Maxwell models), cannot be oscillated instantly; this will take a certain time that is governed by the viscoelastic parameters of the coating material. In [14], an analytical solution for the transient process of establishment of forced vibrations of a single-layer monolithic pliable coating is obtained.

In the first part of this work, pressure pulsations that are measured experimentally are digitally filtered digitally. In the second part, the response of the coating is calculated analytically using the data obtained in the first part of the work.

The signal of the pressure pulsations is recorded on a Schlumberger measuring tape recorder with frequency modulation. The sensor of pressure pulsations has a diameter of the sensitive surface $D \approx 1.5$ mm and is mounted in the zone of developed gradient-free turbulent flow flush with the fairing on the body of revolution under tow (the towing speed is 9 m/sec) [3, 7].

The digital filtration of the signal was performed on a 486-XT personal computer with a developed package of application programs. A standard Vibra 16 sound card was used as the analog-to-digital converter. The signal was digitized in a sixteen-bit regime at one of three discretization frequencies – 11,025, 22,050, and 44,100 conversions per second. The programs were written in the C^{++} programming language, which makes it possible to read data files written by the converter in the *.wav file standard.

Spectral analysis was performed using the Cooley–Tuquit procedure of fast Fourier transformation [15]. To obtain a sufficiently "smooth" spectrum, use was made of averaging over ≈ 250 realizations of this transformation. Figure 2 gives the Fourier spectrum of the pressure pulsations.

Narrow-band filtration was performed using a procedure that realizes a pulsed filter with a finite region of response with a Potter window [15]. A software package processes the signals in the frequency range of 10 Hz to ≈ 20 kHz using the following filtration regimes: octave, 1/3-octave, 1/6-octave, and 1/9-octave regimes. Figure 3 shows the characteristics of the filters. The boundaries of the filters are characterized by a damping of 6 dB. The virtual absence of nonuniformity inside the transmission band and rapid damping higher than 110 dB outside it are noted.

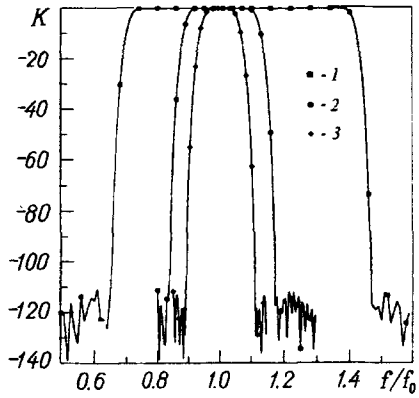

Fig. 3. Characteristics of filters: 1) octave filter; 2) 1/3-octave filter; 3) 1/6-octave filter. K, dB.

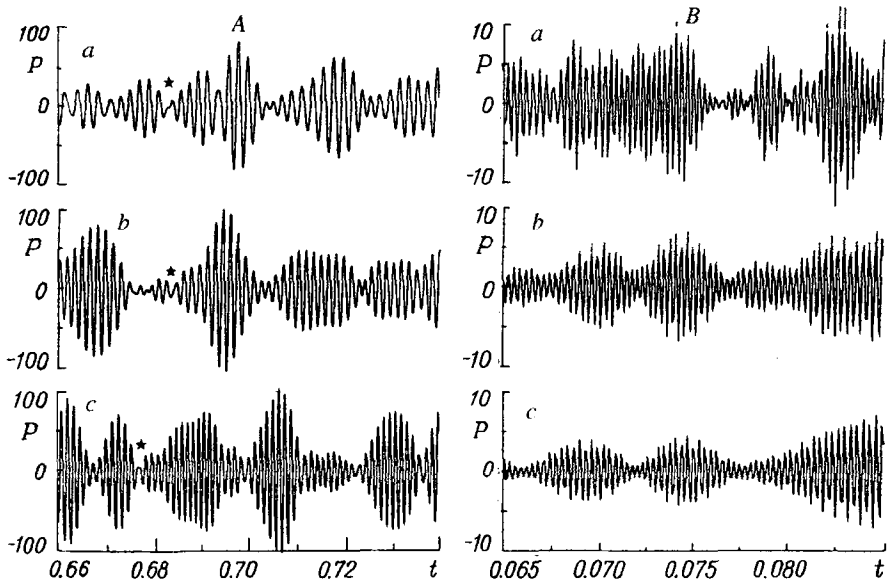

Fig. 4. Examples of realizations: A) 1/3-octave filters [a) f_0 = 500 Hz, b) 630, c) 794]; B) f_0 = 3175 Hz [a) 1/3-octave filter, b) 1/6-octave filter, c) 1/9-octave filter]. t, sec.

Figure 4 gives typical patterns of the signal at the analyzer output. The envelope of the signal from the vortex structure passing by the sensor has the shape of a symmetric meander only in an ideal case (see Fig. 4A, c in the time interval of 0.722 to 0.736 sec). In the general case, we observe combining of signals from several structures. In 1/3-octave filtration, trains of vibrations can be isolated visually for an average filter frequency $f_0 > 500$ Hz. Comparing the envelopes of the signals, we can easily notice a certain correlation of them. At frequencies higher than 1000 Hz, we have to use narrower-band filters to isolate the trains. Thus, Fig. 4B shows that 1/3-octave filtration turns out to be insufficiently efficient while the filter of 1/9 octave already fails to provide additional information compared to the filter of 1/6 octave.

To describe the response of a pliable coating to turbulent pressure pulsations, we must know the magnitude and duration of the portions of their coherent action, i.e., the shape of the envelope of the train and the number of vibrations in it. In the general case, the phase of the vibration changes at the boundaries of the trains. A considerable phase change is marked in Fig. 4A by an asterisk. It should be noted that the duration of quasicoherent action can be larger than one train of vibrations, as is seen from the figures presented.

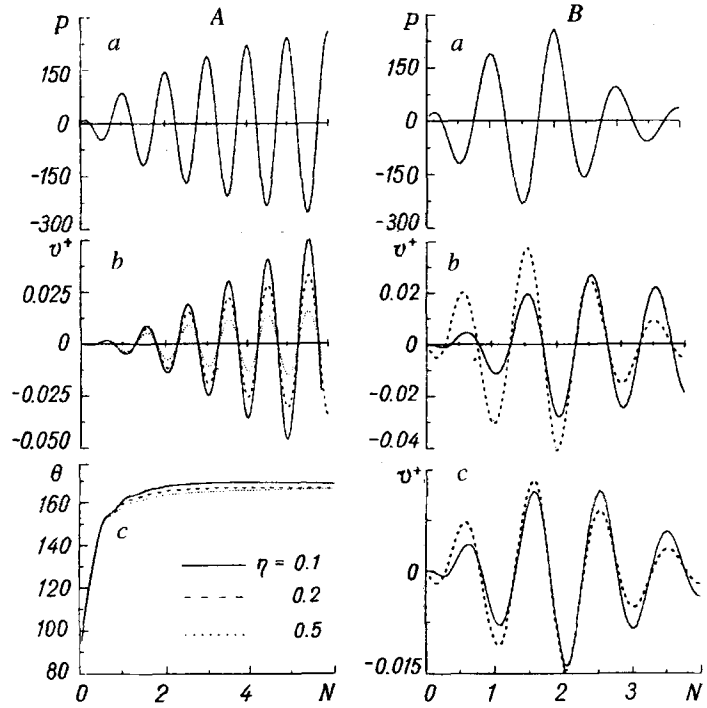

Fig. 5. Response of the coating to a pulsating pressure P that changes by the law: A) $P = P_0 \exp(-t/\tau)$, $\tau = 3$ periods of vibrations: a) pulsating pressure, b) dimensionless velocity of movement of the coating surface v^+, c) phase shift between v^+ and P; B) $P = P_0(1 - \exp(-t/\tau))$ for $0 < N < 2$ and $P_0 \exp(-t/\tau)$ for $2 < N < 4$, $\tau = 1$ period of vibrations: a) pulsating pressure, b) v^+ for $\eta = 0.1$, c) v^+ for $\eta = 0.5$; the dashed curves show v^+ for the "ideal" case of an inertialess coating. P, Pa; θ, deg.

The number of periods of vibrations in a train increases with the filtration frequency and on average is between 5 at a frequency of 600 Hz and 10 at 1.5 Hz. This increase in the number of vibrations in a train is attributable to the fact that the vortex structure, which generates pressure pulsations of different frequency, moves as a single whole with a certain convective velocity.

In [14] it is shown in what manner the time of establishment of forced vibrations of a pliable coating depends on the viscoelastic properties of the coating material. Thus, for a material that has a plateau of the viscoelastic properties (i.e., a weak dependence of the modulus of elasticity E and the loss factor η on the frequency) the vibration amplitude attains a steady state in a certain number of periods of vibrations N that is independent of the parameters of the coating (E, ρ, and H) and is completely governed by its loss factor. At the first resonance frequency of the coating ω, determined by the relation $\omega H\sqrt{\rho/E}(1+\eta^2)^{-1/4} \approx \pi/2$, a level of 0.7 of the steady-state vibrations is attained in $N_{0.7} \approx 10$ for $\eta = 0.1$, which decreases sharply as the loss factor of the coating material increases (thus, $N_{0.7} \approx 1$ for $\eta \approx 0.4$).

However the magnitude of the first resonance peak itself depends on the loss factor, decreasing with increase in it. The buildup rate for the vibration amplitude is approximately the same for different η in the initial period of the relaxation process ($N < 0.5$) and then, for smaller η, becomes larger (Fig. 2a and c from [14]). Therefore the deflection of the surface of a coating with $\eta > 0.8$, which has time to relax in one period of vibrations to the level of 0.95, will follow the shape of the change in the pressure pulsations (the shape of the train) practically without resonance now. There will be another pattern of deformation for coatings manufactured of a material with a small loss factor ($\eta < 0.5$). Since here the relaxation time is larger than one period of vibrations, the time dependence of the deformation of the coating will not follow the shape of the train of

pressure pulsations now but will depend on the number of periods of vibrations in the train. We should emphasize that the amplitude of deformation of the coating surface will increase here.

We calculated analytically the response of the coating to pulsating pressure that changes by the law $P(t) = P_{env} \exp(i\omega t)$, as shown in the upper part of Fig. 5. The frequency ω was selected equal to the first resonance frequency of the coating. The parameters were taken as in an actual coating that showed a reduction in friction and the level of pressure pulsations [3, 7, 8], namely: $E = 5$ MPa, $\rho = 2 \cdot 10^3$ kg/m^3, and $H = 5$ mm. The computational algorithm of [14] was employed. The envelope of the train was simulated by the following exponential dependences: $P_{env} = P_0(1 - \exp(-t/\tau))$ for the portion of growth, $P_{env} = P_0 \exp(-t/\tau)$ for decay.

The characteristic time of change of the pressure pulsations τ, which corresponds approximately to one-fourth of the duration of the train, was selected equal to one, two, and three periods of vibrations.

The dimensionless velocity of movement of the pliable-coating surface is $v^+ = i\omega y(t)/v^*$, where $v^* = \sqrt{\tau_w/\rho_0}$ is the dynamic velocity, $y(t)$ is the vertical movement of the surface, ρ_0 is the density of the liquid. The calculations were performed for a flow velocity of 10 m/sec, $\tau_w \approx 150$ Pa, $v^* = 0.4$ m/sec, and $P_0 \approx 300$ Pa (for a 1/3-octave filter with $f_0 = 1.6$ kHz); P_0 is obtained from the condition of joining of the portions of growth and decay of P_{env}.

Figure 5A shows the pulsating pressure and the response of a pliable coating for the case of an increase in the pulsating pressure by the law $P_0(1 - \exp(-t/\tau))$, where $\tau = 3$ periods of vibrations. As Fig. 5A, c shows, the phase shift between the pulsating pressure applied to the coating and the velocity of movement of the coating surface that is initiated by it relaxes to a constant value $\theta \approx 160$–170° in practically one vibration period independently of the loss factor of the coating material. The dimensionless velocity behaves in a completely different manner. Figure 5A, b shows that although the time in which v^+ attains a steady-state level decreases as η increases, its magnitude itself also decreases.

Figure 5B illustrates the behavior of a pliable boundary for a train of pulsating pressure that consists of four periods of vibrations. At small η the vibrations of the coating surface build up more slowly but attenuate more slowly, too, which leads to asymmetry of the shape of the deformation train (Fig. 5B, b). As has already been mentioned, the dimensionless velocity for a coating with $\eta = 0.1$ is approximately twice that for a coating with $\eta = 0.5$. For comparison, we show v^+ for a the hypothetical case of a zero relaxation time as the dashed curve. Here, the coating surface, under the action of pressure pulsations, would execute forced motions with the amplitude and phase of steady-state vibrations.

The response of an actual coating with a large loss factor (the example for $\eta = 0.5$ is shown in Fig. 5B, c) differs slightly from the reaction of an ideal inertialess coating. As η decreases, the difference is enhanced, which is easily observable in Fig. 5B, b. We also note that on the portions of growth (on the left) the vibration amplitude for the actual coating is smaller than in the hypothetical case, and on the portion of decay (the right parts of Fig. 5B), the reverse applies.

The results obtained show that the coating virtually always operates in the transient regime without attaining the maximum amplitudes of deformations that would occur in the steady-state regime. This difference increases sharply as the number of vibrations in the pressure-pulsation train decreases.

From the condition of continuity of the medium it follows that the rate of deformation of the wall is equal to the normal component of the pulsating velocity of the flow v_0^+ on the wall itself. In the case of a solid boundary, $v_0^+ = 0$ on the surface, increasing to $v_0^+ \approx 1$ at $y^+ = yv^*/\nu \approx 40$, where ν is the kinematic viscosity of water [16]. Since Reynolds stresses are governed by the correlation of the longitudinal and transverse pulsating velocities, the presence of v_0^+ can have a substantial effect on τ_w. Here, we note two special features: the first is that the rate of deformation of the surface and accordingly the additional velocity of the vertical pulsation of the moving medium are practically out of phase with the pulsating pressure, i.e., a positive value of the pulsating pressure corresponds to a negative value of v_0^+ (directed toward the wall) and vice versa; the second is that for the comparatively large value $v_0^+ = 0.05$, the dimensionless movement of the surface does not exceed one viscosity scale, i.e., $y^+ < 1$.

Thus, the analysis performed showed that a resistance reduction is possible on a pliable coating that remains hydrodynamically smooth. The inertia of the coating, which leads to a decrease in the effective defor-

mation, must be taken into account in further development of various theories that explain the change in the parameters of the turbulence in a flow over a pliable coating.

NOTATION

H, thickness of the coating; E, modulus of elasticity; η, loss factor; ρ, density of the coating material; ρ_0, density of the moving medium; f, frequency; $\omega = 2\pi f$, cyclic frequency; t, current time; f_0, average frequency of the filter; τ_w, tangential stress on the wall; τ, characteristic time of change of the harmonic of pressure pulsations; P_0, amplitude of the pulsating pressure after filtration; P_{env}, envelope of the train of pressure pulsations; N, number of vibrations in the train; y, deformation of the coating surface; y^+, dimensionless deformation of the coating surface; u, longitudinal component of the pulsating velocity; v, component of the pulsating velocity normal to the wall; v^+, dimensionless velocity of movement of the coating surface; v_0^+, normal component of the pulsating velocity of the flow; v^*, dynamic velocity; U_c, convective velocity; θ, phase shift; K, transmission coefficient of the filter.

REFERENCES

1. M. O. Kramer, *J. Amer. Soc. Naval Eng.*, **72**, 25-33 (1960).
2. T. B. Benjamin, *J. Fluid Mech.*, **16**, 436-450 (1963).
3. V. M. Kulik, I. S. Poguda, and B. N. Semenov, in: *Recent Developments in Turbulence Management*, Kluwer (1991), pp. 263-283.
4. J. H. Duncan, A. M. Waxman, and M. P. Tulin, *J. Fluid Mech.*, **158**, 117-197 (1985).
5. B. N. Semenov and A. V. Semenova, in: *Proc. Int. Symp. Seawater Drag Reduction*, Newport (1996), pp. 189-195.
6. T. Lee, M. Fisher, and W. H. Schwarz, *J. Fluid. Mech.*, **288**, 37-58 (1995).
7. V. M. Kulik, I. S. Poguda, and B. N. Semenov, *Inzh.-Fiz. Zh.*, **47**, No. 2, 189-196 (1984).
8. K.-S. Choi, X. Yang, B. R. Clayton, E. J. Glover, M. Atlar, B. N. Semenov, and V. M. Kulik, in: *Proc. Roy. Soc.* (London), Ser. A, **454**, 2229-2240 (1997).
9. V. M. Kulik, in: *BIONA Report 12* (1998), pp. 225-229.
10. V. N. Semenov, in: *Emerging Techniques in Drag Reduction*, London (1996), pp. 240-251.
11. V. P. Reutov and G. V. Rybushkina, *Phys. Fluids*, **10**, No. 2, 417-425 (1998).
12. W. W. Willmarth, *Adv. Appl. Mech.*, **15**, 159-254 (1975).
13. J. H. Duncan, *J. Fluid Mech.*, **171**, 339-363 (1986).
14. V. M. Kulik, S. L. Morozova, and L. V. Kulik, *Inzh.-Fiz. Zh.*, **71**, No. 4, 652-656 (1998).
15. R. Otnes and L. Enokson, *Applied Analysis of Time Series. Basic Methods* [Russian translation], Moscow (1982).
16. E. M. Khabakhpasheva and B. V. Perepelitsa, *Inzh.-Fiz. Zh.*, **14**, No. 4, 598-601 (1968).